Dual Targeting of Angipoietin-1 and von Willebrand Factor by microRNA-671-5p Attenuates Liver Angiogenesis and Fibrosis

Le Yang,[1] Wenhui Yue,[1] Hang Zhang,[1] Zhi Zhang,[1] Renmin Xue,[1] Chengbin Dong,[2] Fuquan Liu,[2] Na Chang,[1] Lin Yang,[1] and Liying Li [iD] [1]

Angiopoietin-1 (Angpt1) and von Willebrand factor (VWF) are two important angiogenic molecules that can drive pathologic angiogenesis and progression of liver fibrosis in our previous study. MicroRNAs (miRs) participate in a variety of physiological and pathological processes, including angiogenesis. However, the critical miRs targeting Angpt1 or VWF and potential molecular mechanism underlying liver fibrosis–associated angiogenesis is not clear yet. Human liver tissues were obtained from patients with different chronic liver diseases. Mouse models of liver fibrosis were induced by injection of CCl_4 or bile duct ligation (BDL) operation. MiR-671-5p was predicted to target Angpt1 and VWF from three databases (miRanda, RNA22v2, and miRwalk). MiR-671-5p expression was decreased in the fibrotic liver of human and mice, with a negative correlation with the levels of Angpt1, VWF, sphingosine kinase-1 (SphK1, the rate-limiting enzyme for sphingosine 1-phosphate [S1P] formation), transforming growth factor β1 (TGFβ1), hypoxia inducible factor (Hif)1α, Hif2α, and fibrosis markers. Importantly, miR-671-5p expression was down-regulated in fluorescence-activated cell sorted liver sinusoidal endothelial cells and hepatic stellate cells (HSCs) in CCl_4 mice compared with control mice. *In vitro* miR-671-5p expression was also decreased in S1P-stimulated HSCs and TGFβ1-activated liver sinusoidal endothelial cells, negatively correlated with Angpt1 and VWF expression. MiR-671-5p directly targeted Angpt1 and VWF by luciferase reporter assays. *In vivo* administration of miR-671-5p agomir decreased the messenger RNA and protein levels of Anpgt1 and VWF, and attenuated CCl_4-induced or BDL-induced liver angiogenesis and fibrosis. *Conclusion:* We identify the negative regulation of miR-671-5p on Angpt1 and VWF and liver fibrosis–associated angiogenesis, which may provide promising targets for the prevention and treatment of liver disease. (*Hepatology Communications* 2022;6:1425-1442).

L iver fibrosis is a complicated wound-healing response to tissue injury from a wide variety of etiologies, which might eventually lead to cirrhosis, portal hypertension and liver failure, and represents the main risk factor for hepatocellular carcinoma.[1] Liver fibrosis is characterized by the excessive deposition of extracellular matrix components, increased angiogenesis, and the development of

abnormal angioarchitecture in the liver.[2] Therefore, targeting the key molecules involved in the development of liver fibrosis–associated angiogenesis is viewed as a promising intervention strategy for liver diseases.

Angiopoietin-1 (Angpt1), produced by pericytes and vascular smooth muscle cells, is a critical factor for vascular morphogenesis and function in various development, homeostasis, and disease.[3] For instance, Angpt1 induces vessel stabilization by inhibiting the permeability of endothelial cells and stimulating endothelial cell–dependent release of cytokines such as platelet-derived growth factor-B, which result in the recruitment of pericytes to the nascent vessels.[4] Von Willebrand factor (VWF) is another important angiogenic molecule, which is best known in the regulation of angiogenesis.[5] VWF is selectively expressed in endothelial cells, and VWF expression is up-regulated by angiogenic factors vascular endothelial growth factor, fibroblast growth factor-2, and transforming growth factor β (TGFβ).[6] The deficiency or defect of VWF in human would lead to von Willebrand disease, characterized by a wide range of bleeding disorders (e.g., epistaxis, gingival bleeding, heavy menstrual bleeding, gastrointestinal bleeds, postoperative bleeding, hemarthrosis).[7] Our previous study has demonstrated that Angpt1, which is induced by sphingosine 1-phosphate (S1P) in hepatic stellate cells (HSCs) and VWF in liver sinusoidal endothelial cells (LSECs), drive pathologic angiogenesis and progression of liver fibrogenesis in CCl_4 mouse fibrotic models, and inhibition of Angpt1-mediated angiogenesis results in the attenuation of hepatic fibrosis.[8] However, the critical regulator and potential molecular mechanism underlying the angiogenic process in liver fibrosis is not yet fully understood.

MicroRNAs (miRs) are single-stranded small (~21-25 nucleotides) noncoding RNAs that suppress the expression of target genes by base-pairing with the 3′-untranslated region (3′-UTR) of their target messenger RNAs (mRNAs).[9-11] MiRNAs have been demonstrated to participate in a variety of physiological and pathological processes, including angiogenesis.[12,13] Deregulation of miRNAs has been shown to result in aberrant gene expression and regulate the progression of angiogenesis in liver.[14,15] For instance, miRNA-26a inhibits tumor angiogenesis of human hepatocellular carcinoma through the hepatocyte growth factor–cMet signaling pathway.[16] MiR-195 suppresses angiogenesis and metastasis of hepatocellular carcinoma by inhibiting the expression of vascular endothelial growth factor, vav guanine nucleotide exchange factor 2, and CDC42.[17] Exosomal miR-25-3p from colorectal cancer dramatically induces vascular leakiness and enhances tumor metastasis in liver and lung of mice by targeting Kruppel-like factor 2 and 4.[18] Our previous study has demonstrated that miR-26b-5p inhibits liver fibrogenesis and angiogenesis by directly targeting platelet-derived growth factor receptor-β and interacting with long noncoding RNA MEG3 in mesenchymal stromal cells.[19] However, the critical miRs targeting Angpt1 and VWF, which are the most important regulatory molecules during liver fibrosis-associated angiogenesis, are still not clear.

In the present study, we investigate the potential regulatory mechanism of miR-671-5p on Angpt1

ARTICLE INFORMATION:

From the [1]Department of Cell Biology, Municipal Laboratory for Liver Protection and Regulation of Regeneration, Capital Medical University, Beijing, China; [2]Department of Interventional Therapy, Beijing Shijitan Hospital, Capital Medical University, Beijing, China.

ADDRESS CORRESPONDENCE AND REPRINT REQUESTS TO:

Liying Li, Ph.D.
Department of Cell Biology
Municipal Laboratory for Liver Protection and Regulation of
Regeneration

Capital Medical University
No.10 Xitoutiao, You An Men, Beijing 100069 P. R. China
E-mail: liliying@ccmu.edu.cn
Tel.: +0086-10-83950468

and VWF during liver fibrosis–associated angiogenesis both *in vivo* and *in vitro*. Our data contribute to the understanding of molecular mechanism underlying liver fibrosis–associated angiogenesis and indicate miR-671-5p/Angpt1 and miR-671-5p/VWF as promising targets for the treatment of liver disease.

Materials and Methods

MOUSE MODELS

Mouse models of liver fibrosis were induced by injection of CCl_4 or bile duct ligation (BDL) operation. Male ICR mice aged 6 weeks received intraperitoneal injections of 1 μL/g body weight of a CCl_4/olive oil (OO) mixture, 1:9 vol/vol, twice per week. Mice were sacrificed at 1, 2, 7, or 28 days of CCl_4 treatment, always on the day after the last injection. Another liver fibrosis model of mice was allocated randomly to two experimental groups, either BDL or sham operations, and performed as described previously.[20] Liver tissue was collected for quantitative real-time polymerase chain reaction (PCR), western blot, immunofluorescence analysis, and sirius red staining.

MiR-671-5p agomir (miR-671-5p mimic *in vivo*) was purchased from Guangzhou RiboBio and was delivered *in vivo* using a "hydrodynamic transfection method," in which 5 nmol or 10 nmol miR-671-5p agomir was rapidly injected into the tail vein of each mouse. Control mice were injected with an equal volume of control agomir dissolved in phosphate buffered saline. These miR agomirs were injected twice per week in CCl_4-treated mice for 4 weeks or BDL mice for 1 week. All animals received human care, and all animal protocols were conformed to the Ethics Committee of Capital Medical University and in accordance with the approved guidelines (approval number AEEI-2014-131).

HUMAN LIVER SPECIMEN

Human fibrotic samples (fibrosis stage F2-F4) were obtained from livers of 20 patients undergoing liver biopsy (12 men, 8 women; mean age: 58 years; range: 25-76 years). Fibrosis was consecutive to chronic hepatitis B virus (HBV; n = 3), hepatitis C virus (HCV; n = 3), alcohol-associated liver disease (n = 4), cryptogenic liver disease (n = 3), cholestatic liver disease (n = 3), drug-induced liver disease (n = 1), and autoimmune liver disease (n = 3). Normal liver samples were collected from 6 patients undergoing hepatic resection for hepatic hemangioma. All subjects gave their informed consent for inclusion before they participated in the study. The study was conducted in accordance with the Declaration of Helsinki, and the protocol was approved by the Ethics Committee of Beijing Shijitan Hospital, Capital Medical University, Beijing, China (project identification code 2018EC-1).

ISOLATION AND CULTURE OF PRIMARY MOUSE HSCs

Primary mouse HSCs were isolated from adult male ICR mice by collagenase perfusion and purified by density gradient in Nicodenz (AXIS-SHIELD PoC; Scotland). LSECs were purchased from Bluefbio Biology Technology Company (China).

IMMUNOFLUORESCENCE STAINING

Liver samples were fixed in 4% paraformaldehyde and embedded in Tissue Tek OCT compound. Five micrometers of frozen section were used for immunofluorescence. The liver sections were blocked with 2% bovine serum albumin, and then incubated with anti-CD31 polyclonal antibody (1:50; BD Pharmingen, Franklin Lakes, NJ) and Cy3-conjugated AffiniPure goat anti-rabbit immunoglobulin G antibody (1:100; Jackson Immunoresearch, West Grove, PA) as a secondary antibody. The samples were covered with Vectashield mounting medium containing 4′,6-diamidino-2-phenylindole and observed under confocal microscope (LSM510; Carl Zeiss MicroImaging GmbH, Germany).

QUANTITATIVE REAL-TIME PCR

Total RNA was extracted from cultured HSCs, LSECs, and liver tissue using RNeasy kit (Qiagen, Hilden, Germany). Real-time reverse-transcription PCR was performed in an ABIPrism 7300 sequence detecting system (Applied Biosystems, Foster City, CA). Primers were as follows: 18SrRNA: sense, 5′-GTA ACC CGT TGA ACC CCA TT-3′; antisense, 5′-CCA TCC AAT CGG TAG CG-3′. Mouse Angpt1: sense, 5′-GGA TGT GCT GTC

TAG GCA GAA-3′; antisense, 5′-TTC ATG TTC CGG CTT TCC TTT-3′. Mouse VWF: sense, 5′-GCG CTA TCA TGT ATG AAG TCA GGT T-3′; antisense, 5′-CAC AGA TTC CGC AAA GAC CAT-3′. Mouse TGFβ1: sense, 5′-TGC GCT TGC AGA GAT TAA AA-3′; antisense, 5′-TCA CTG GAG TTG TAC GGC AG-3′. Mouse sphingosine kinase-1 (SphK1): sense, 5′-TGT CAC CCA TGA ACC TGC TGT CCC TGC ACA-3′; anti-sense, 5′-AGA AGG CAC TGG CTC CAG AGG AAC AAG-3′. Mouse α-smooth muscle actin (α-SMA): sense, 5′-ATG CTC CCA GGG CTG TTT T-3′; antisense, 5′-TTC CAA CCA TTA CTC CCT GAT GT-3′. Mouse procollagen α1(I) (Colα1[I]): sense, 5′-AGG GCG AGT GCT GTG CTT T-3′; antisense, 5′-CCC TCG ACT CCT ACA TCT GA-3′. Mouse procollagen α1(III) (Colα1[III]): sense, 5′-TGA AAC CCC AGC AAA ACA AAA-3′; antisense, 5′-TCA CTT GCA CTG GTT GAT AAG ATT AA-3′. Mouse hypoxia inducible factor 1α (Hif1α): sense, 5′-ACC TTC ATC GGA AAC TCC AAA G-3′; antisense, 5′-ACT GTT AGG CTC AGG TGA ACT-3′. Mouse Hif2α: sense, 5′-CTG AGG AAG GAG AAA TCC CGT-3′; antisense, 5′-TGT GTC CGA AGG AAG CTG ATG-3′. Mouse vascular endothelial growth factor α (VEGFα): sense, 5′-CTG CCG TCC GAT TGA GAC C-3′; antisense, 5′-CCC CTC CTT GTA CCA CTG TC-3′. Mouse tek receptor tyrosine kinase (Tie2): sense, 5′-GAG TCA GCT TGC TCC TTT ATG G-3′; antisense; 5′-AGA CAC AAG AGG TAG GGA ATT GA-3′. Mouse fibroblast growth factor (FGF): 5′-CCC TGA CCG AGA GGT TCA AC-3′; antisense; 5′-GTC CCT TGT CCC ATC CAC G-3′. Human Angpt1: sense, 5′-GGA AGG GAA CCG AGC CTA TT-3′; antisense, 5′-TTC CTG TCC CAG TGT GA-3′. Human VWF: sense, 5′-GAG TGA CAG TGT TCC CTA TTG GAA-3′; antisense, 5′-TCT TCG ATT CGC TGG AGC TT-3′. Human TGFβ1: sense, 5′-AGT TCA AGC AGA GTA CAC ACA GCA T-3′; antisense, 5′-AGA GCA ACA CGG GTT CAG GTA-3′. Human SphK1: sense, 5′-GCT CTG GTG GTC ATG TCT GG-3′; antisense, 5′-CAC AGC AAT AGC GTG CAG T-3′. Human α-SMA: sense, 5′-CTG GCA TCG TGC TGG ACT CT-3′; antisense, 5′′-GAT CTC GGC CAG CCA GAT C-3′. Human Colα1(I): sense, 5′-AGG AAG GGC CAC GAC AAA G-3′;

antisense, 5′-ACA CAG TTA CAC AAG GAA CAG AAC AGT-3′. Human Colα1(III): sense, 5′-GGG AAT GGA GCA AAA CAG TCT T-3′; antisense, 5′-CCA ACG TCC ACA CCA AAT TCT-3′. Human Hif1α: sense, 5′-GAA CGT CGA AAA GAA AAG TCT CG-3′; antisense, 5′-CCT TAT CAA GAT GCG AAC TCA CA-3′. Human Hif2α: sense, 5′-CGG AGG TGT TCT ATG AGC TGG-3′; antisense, 5′-AGC TTG TGT GTT CGC AGG AA-3′.

WESTERN BLOT ANALYSIS

Western blot analysis of Angpt1 was performed with 50 μg of protein extract using polyclonal antibodies to Angpt1 (1:100; Abcam, Cambridge, United Kingdom), VWF (1:1,000; ABclonal, China), and the appropriate IRDyeTM 800-conjugated secondary antibody (1:10,000). Signals were detected using the Odyssey Imaging System (LI-COR Biosciences, Lincoln, NE) and analyzed with Odyssey software. Results were normalized relative to the glyceraldehyde-3-phosphate dehydrogenase (GAPDH) (rabbit anti-GAPDH monoclonal antibody, 1:1,000; Sigma-Aldrich, St. Louis, MO) expression to correct for variations in protein loading and transfer.

FLUORESCENCE-ACTIVATED CELL SORTING

Liver nonparenchymal cells were isolated from mouse liver as previously described.[21] Subsequently, antibodies (Brilliant Violet 421-CD31 [BioLegend, San Diego, CA] and PE-PDGFRβ [BioLegend]) and their isotype-matched negative control antibodies were added to the cell suspension. After 30 minutes of incubation in the dark, the cells were washed with phosphate-buffered saline and subjected to fluorescence-activated cell sorting (FACS), which was performed on FACSAria IIIu and analyzed with FACSDiva software v8.0 (BD Biosciences, Franklin Lakes, NJ).

HISTOLOGY ANALYSIS

Liver paraffin sections (5 μm) were stained with sirius red for collagen visualization. The fibrotic areas were assessed using the software Image-Pro Plus. The mean value of 15 randomly selected areas per sample was used as the expressed percentage of fibrotic areas.

LUCIFERASE REPORTER ASSAYS

Cells were seeded in 96-well plates for 24 hours, then subsequently co-transfected with 5 ng wild-type or mutant reporter plasmid (Guangzhou RiboBio, China) and 50 nM miR-671-5p mimic or miR-control using Lipofectamine 2000. Firefly and Renilla luciferase activities were measured 48 hours after transfection using the Dual Luciferase Assay (Promega, Madison, WI), according to the manufacturer's protocol. Firefly luciferase activity was normalized to Renilla, and the value of Firefly luciferase activity/Renilla luciferase activity was analyzed.

MiR PREDICTION

To identify the miRNAs targeting Angpt1 and VWF, we predicted miRNAs from databases (www.microrna.org/microrna/home.do, https://cm.jefferson.edu/rna22/, http://mirwalk.umm.uni-heidelberg.de/) that combine thermodynamics-based modeling of RNA: RNA duplex interactions with comparative sequence analysis to predict miR targets conserved across multiple genomes according to the structures, energies, and scoring.

STATISTICAL ANALYSIS

The results were expressed as mean ± SEM. Statistical analyses were carried out using a Statistical Package for Social Sciences (SPSS, version 17.0) software. A two-sided Student t test was used to analyze differences between two groups, and one-way analysis of variance followed by a *post hoc* LSD test was used when more than two groups were compared. Correlation coefficients were calculated by Pearson test. $P < 0.05$ was considered to be statistically significant ($*P < 0.05$; $**P < 0.01$; $^{#}P < 0.05$; $^{##}P < 0.01$). All results were verified in at least three independent experiments.

Results

MiR-671-5p EXPRESSION WAS DECREASED IN THE FIBROTIC LIVER OF MICE AND HUMAN, WITH NEGATIVE CORRELATIONS TO Angpt1 AND VWF LEVELS

Angpt1 and VWF had been proved to be critical factors driving pathologic angiogenesis and liver fibrosis by our previous study.[8] To explore the potential molecular mechanism underlying liver fibrosis–associated angiogenic process, we screened potential miRs targeting these two key molecules involved in angiogenesis from an intersection of three prediction databases (miRwalk, miRanda, and RNA22v2), and chose miR-671-5p as our candidate to focus on its regulation on angiogenesis during liver fibrosis in the following study. The binding sites of miR-671-5p in the 3′-UTR of Angpt1 and VWF mRNAs are shown (Fig. 1A). The hepatic expression of miR-671-5p continuously reduced in a time-dependent manner throughout the entire stage of liver injury in CCl_4-treated mice (Fig. 1B). We then analyzed the correlation between the hepatic levels of miR-671-5p and its potential targets Angpt1 and VWF. A straight-line fit was obtained between the expression of miR-671-5p and Angpt1 (Fig. 1C, left), miR-671-5p, and VWF (Fig. 1C right) in mouse liver, indicating that there was a close relationship among them.

We also tested the expression of miR-671-5p in patient liver tissue of different etiologies, including chronic HBV and HCV infections, alcohol abuse, drug-induced liver disease, and autoimmune liver disease. Our results showed a remarkable decrease of miR-671-5p expression in the fibrotic liver of patients compared with that in normal liver tissue (Fig. 1D). A negative correlation between miR-671-5p and the mRNA expression of Angpt1 (Fig. 1E left) and VWF (Fig. 1E right) was obtained in human liver as well. Because angiogenesis was usually activated by hypoxia,[22] we further measured the expression of Hif1α and Hif2α, and analyzed their correlation with miR-671-5p levels in liver. The results showed a negative correlation between the levels of miR-671-5p and Hif1α or Hif2α in mouse and human liver (Table 1). Taken together, these results showed a correlation between the expression of miR-671-5p and Angpt1, and miR-671-5p and VWF, in both human and mouse liver, indicating the potential regulation of miR-671-5p on angiogenesis during liver injury.

In addition, FACS was performed to sort quiescent HSC (vitamin A⁺), activated HSC (PDGFRβ⁺), and EC/LSEC (CD31⁺) among liver nonparenchymal cells (Fig. 2A). Sorted vitamin A⁺ cells were detected by light and fluorescent microscopy for vitamin A expression after adherence for 5 hours
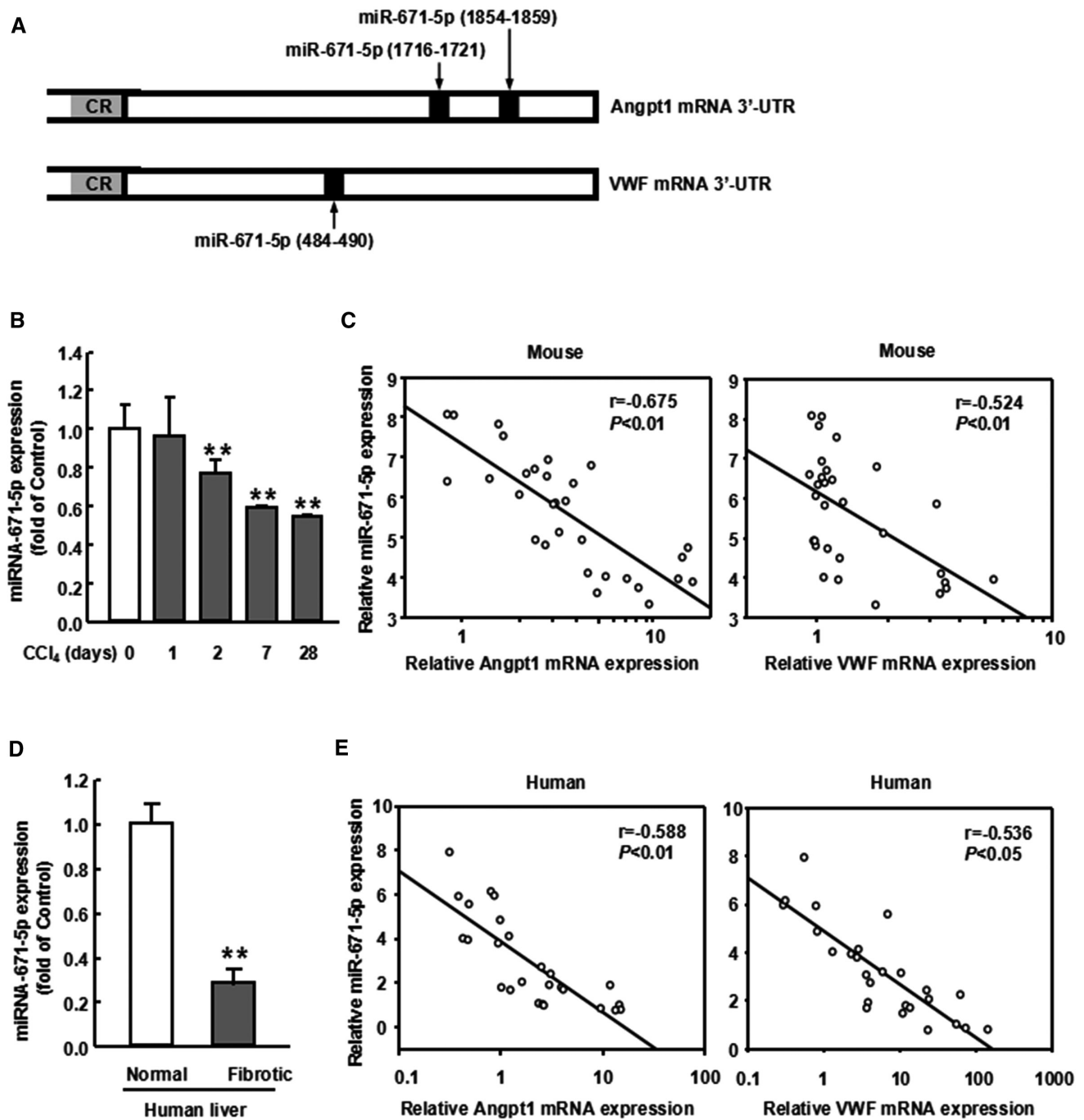
FIG. 1. Expression of miR-671-5p and its correlation with Angpt1 or VWF in human and mouse liver. (A) The miR-671-5p binding sites in the 3′-UTR of Angpt1 or VWF mRNA. (B) MiR-671-5p expression in CCl_4-treated fibrotic liver. (C) The correlation between miR-671-5p and Angpt1, and miR-671-5p and VWF, in mouse liver. (D) MiR-671-5p expression in the fibrotic liver of patients. (E) Correlation between miR-671-5p and Angpt1, and miR-671-5p and VWF, in human liver. Data are presented as the mean ± SEM (n = 6 per group). All results were verified in at least three independent experiments. **$P < 0.01$ versus control.

and paraformaldehyde fixation (Fig. 2A). The levels of miR-671-5p in sorted HSC and EC/LSEC of fibrotic livers were examined by quantitative real-time PCR. The results showed that miR-671-5p expression was decreased in EC/LSEC (by 21%) and HSC (by 8%) in CCl_4 mice compared with control mice,

TABLE 1. CORRELATION BETWEEN miR-671-5p AND SphK1, TGFβ1, FIBROSIS MARKERS, AND HIF FAMILY MEMBERS IN MOUSE AND HUMAN LIVER

		Gene	Correlation Coefficients (r)	P Value
Mouse		SphK1	–0.832	<0.01
		TGFβ1	–0.532	<0.01
	Fibrosis markers	α-SMA	–0.697	<0.01
		Col α1(I)	–0.622	<0.01
		Col α1(III)	–0.775	<0.01
	Hif	Hif1α	–0.554	<0.01
		Hif2α	–0.431	<0.05
Human		SphK1	–0.662	<0.01
		TGFβ1	–0.480	<0.05
	Fibrosis markers	α-SMA	–0.605	<0.01
		Col α1(I)	–0.540	<0.05
		Col α1(III)	–0.565	<0.01
	Hif	Hif1α	–0.578	<0.01
		Hif2α	–0.619	<0.01

Note: The hepatic expression of miR-671-5p and SphK1 (the rate-limiting enzyme for S1P formation), TGFβ1, fibrosis markers (α-SMA, Col α1[I], and Col α1[III]), and Hif family members was quantified using quantitative real-time PCR. The relationship between miR-671-5p and SphK1, TGFβ1, fibrosis markers, Hif1α and Hif2α was analyzed by regression analysis (n = 30 for mice, n = 20 for patients).

further verifying the critical role of miR-671-5p in these two cell types (Fig. 2B).

MiR-671-5p EXPRESSION WAS DECREASED IN ACTIVATED HSCs AND LSECs, WITH A NEGATIVE CORRELATION TO Angpt1 AND VWF EXPRESSION

S1P is a bioactive lipid mediator that can regulate many physiological processes, including angiogenesis and vascular permeability.[23] Our previous study has shown that S1P could induce the expression of Angpt1 in HSCs, leading to the formation of pathological angiogenesis and progression of liver fibrosis in mouse models of liver injury.[8] We then analyzed the correlation between the hepatic levels of miR-671-5p and the rate-limiting enzyme for S1P formation, SphK1.[24] A negative correlation between the expression of miR-671-5p and SphK1 was obtained in both mouse and human liver (Table 1), indicating that S1P might be a potent mediator in the regulation of miR-671-5p on angiogenesis during liver injury. Based on

the critical role of S1P in angiogenesis and the close relationship between miR-671-5p and S1P in injured liver (Table 1), primary HSCs were stimulated with different concentrations of S1P. The expression of miR-671-5p displayed a decrease in a dose-dependent manner after S1P stimulation in HSCs (Fig. 3A, left), whereas miR-671-5p expression was almost unchanged under the treatment of TGFβ1 in HSCs (Fig. 3A, right). Angpt1 expression was up-regulated in S1P-treated cells (Fig. 3B), showing a negative correlation between the expression of miR-671-5p and its potential target Angpt1 (Fig. 3E).

VWF, an angiognic molecule produced by endothelial cells, plays a pivotal role in the modulation of angiogenesis.[6] Next, we explored the regulatory effect of miR-671-5p on VWF mRNA expression in TGFβ1-activated LSECs. We analyzed the correlation between the hepatic levels of miR-671-5p and TGFβ1, showing a negative correlation between them in the liver of mice and human (Table 1). Furthermore, TGFβ1 stimulation reduced the expression of miR-671-5p in LSECs (Fig. 3C, right), whereas S1P had no obvious effect on miR-671-5p level in LSECs (Fig. 3C, left). TGFβ1 stimulation also increased the expression of VWF in cultured LSECs (Fig. 3D), displaying a negative correlation between them (Fig. 3F). Altogether, these results suggest that miR-671-5p might be a potential regulator targeting both Angpt1 and VWF in activated HSCs and LSECs during liver fibrosis-associated angiogenesis.

MiR-671-5p DIRECTLY TARGETED Angpt1 AND VWF IN HSCs AND LSECs

To confirm that Angpt1 and VWF were directly targeted and regulated by miR-671-5p, HSCs and LSECs were transfected with miR-671-5p mimic or inhibitor to alter its expression, respectively, and the transfected efficiency was verified by quantitative real-time PCR analysis (Fig. 4A,C,E,G). Overexpression of miR-671-5p with its mimic inhibited the S1P-induced increase of Angpt1 mRNA expression in HSCs (Fig. 4B), whereas miR-671-5p inhibition resulted in the up-regulation of Angpt1 (Fig. 4D). Consistently, transfection of miR-671-5p mimics in LSECs suppressed the TGFβ1-induced increase of VWF mRNA expression (Fig. 4F), while miR-671-5p inhibitor showed the opposite effect (Fig. 4H).
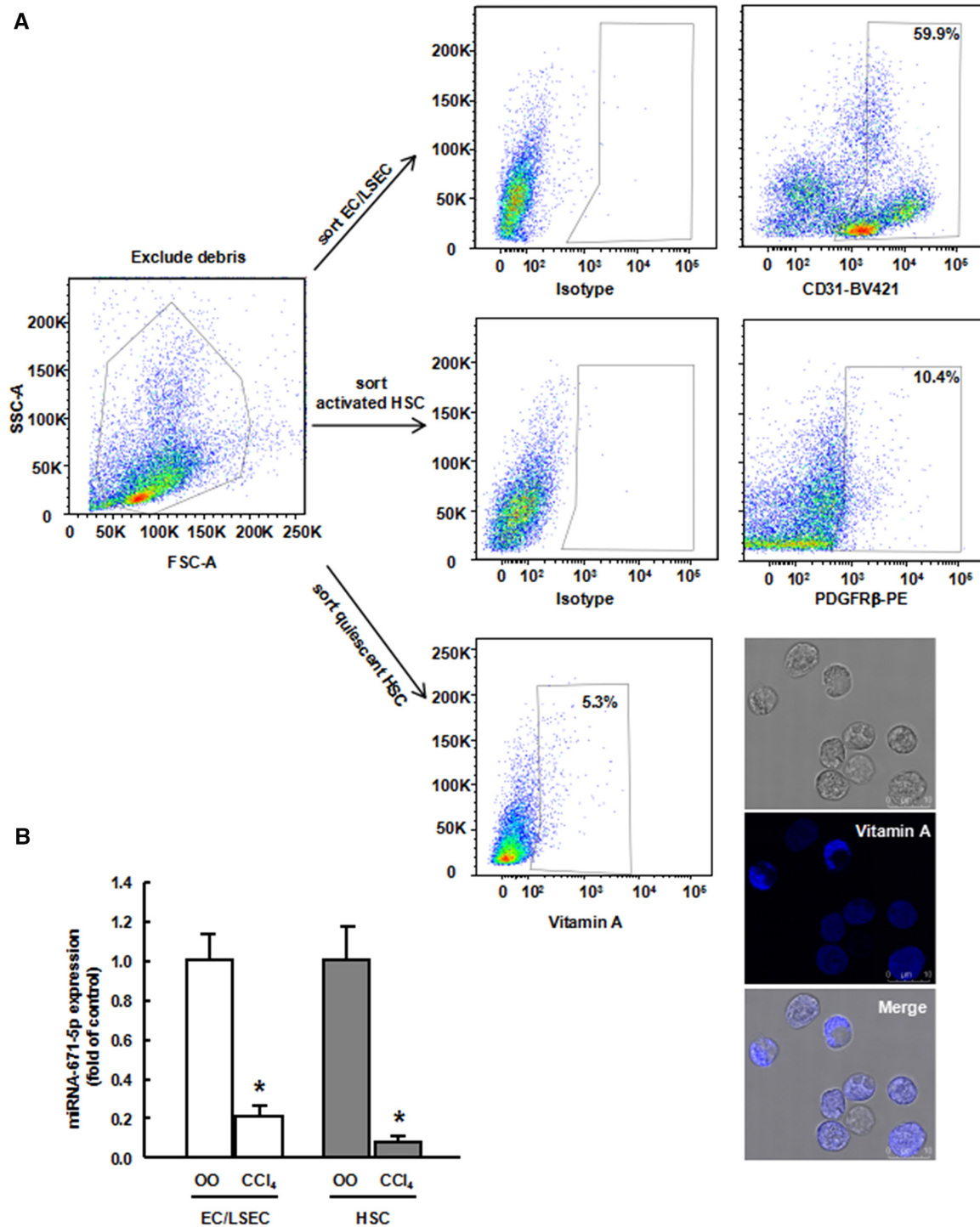
FIG. 2. Expression of miR-671-5p in sorted HSCs and EC/LSECs. FACS was performed to sort HSC (vitamin A$^+$, PDGFRβ$^+$) and EC/LSEC (CD31$^+$) among liver nonparenchymal cells using BD FACSAria IIIu. (A) FACS dot blots show the sorting gates for EC/LSECs and HSCs from liver nonparenchymal cells. EC/LSECs were defined as CD31$^+$ cells, and HSCs were defined as vitamin A$^+$ or PDGFRβ$^+$ cells. Sorted vitamin A$^+$ cells were detected by light and fluorescent microscopy. (B) Expression of miR-671-5p in sorted HSCs and EC/LSECs of CCl$_4$ mice. Data are presented as the mean ± SEM (n = 6 per group). All results were verified in at least three independent experiments. $^*P < 0.05$ versus control.
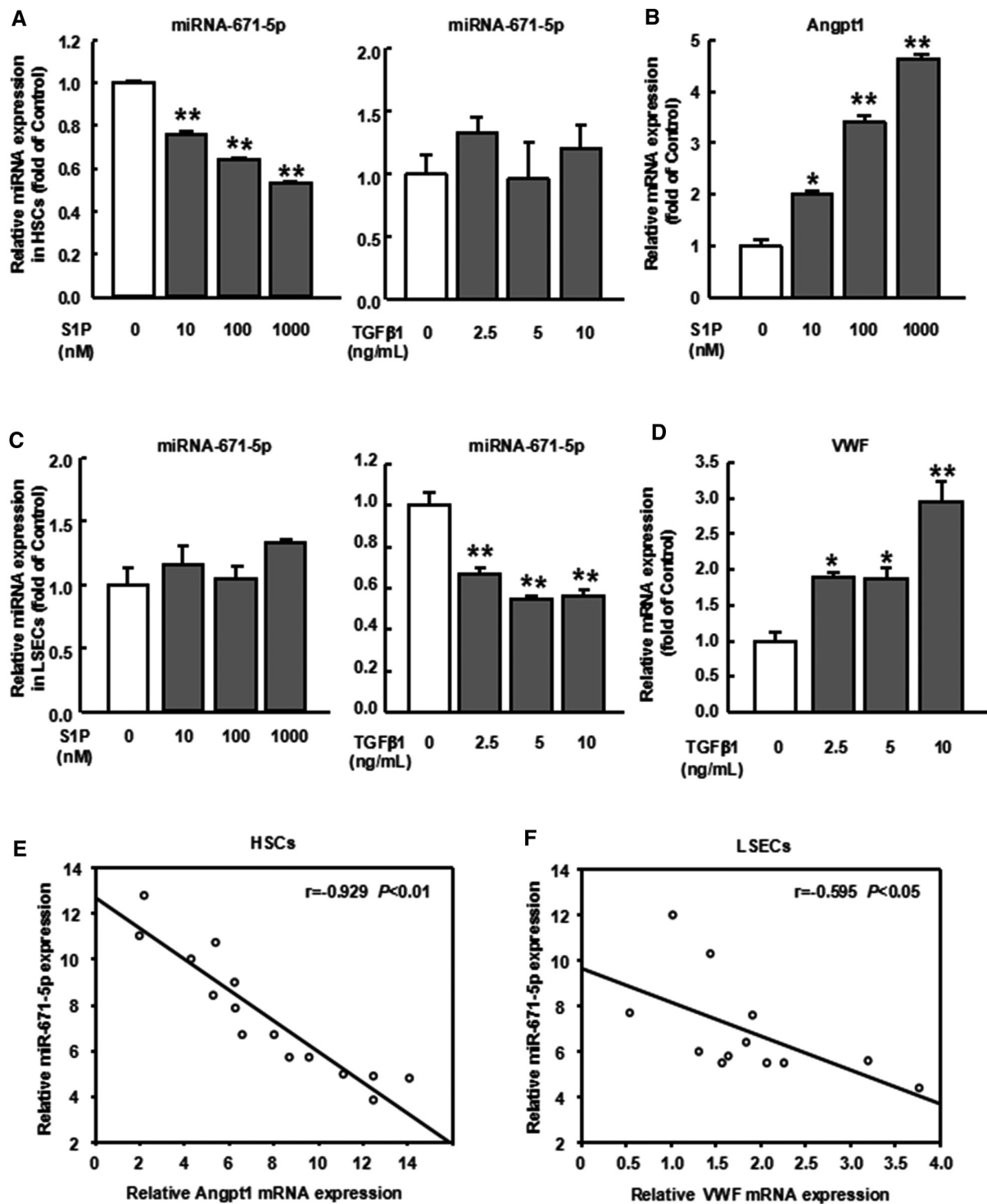
FIG. 3. Expression of miR-671-5p and its correlation with Angpt1 or VWF expression in HSCs and LSECs. HSCs or LSECs were treated with different concentration of S1P for 6 hours or TGFβ1 for 24 hours to examine the expression of Angpt1, VWF, and miR-671-5p. (A) MiR-671-5p expression in S1P-treated or TGFβ1-treated HSCs. (B) Angpt1 expression in S1P-treated HSCs. (C) MiR-671-5p expression in S1P-treated or TGFβ1-treated LSECs. (D) VWF expression in TGFβ1-treated LSECs. (E) Correlation between miR-671-5p and Angpt1 in HSCs. (F) Correlation between miR-671-5p and VWF in LSECs. Data are presented as the mean ± SEM (n = 3 per group). All results were verified in at least three independent experiments. $^{*}P < 0.05$ versus control; $^{**}P < 0.01$ versus control.
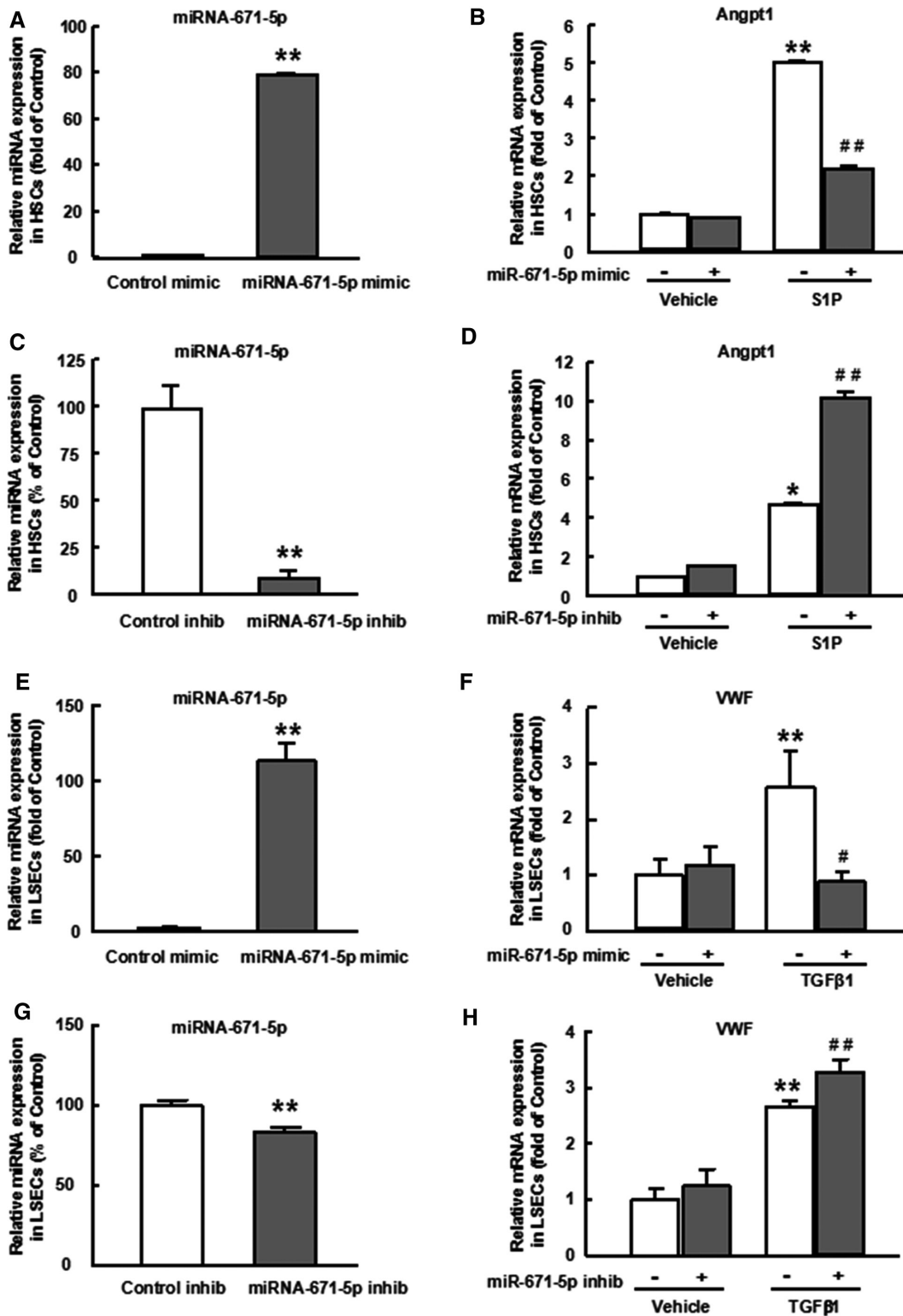
FIG. 4. MiR-671-5p directly targeted Angpt1 and VWF in HSCs and LSECs. (A) Transfection efficiency of miR-671-5p mimic in HSCs. (B) Angpt1 mRNA expression was examined by quantitative real-time PCR with the transfection of miR-671-5p mimic in HSCs. (C) Transfection efficiency of miR-671-5p inhibitor in HSCs. (D) Angpt1 mRNA expression was examined by quantitative real-time PCR with the transfection of miR-671-5p inhibitor in HSCs. (E) Transfection efficiency of miR-671-5p mimic in LSECs. (F) VWF mRNA expression was examined by quantitative real-time PCR with the transfection of miR-671-5p mimic in LSECs. (G) Transfection efficiency of miR-671-5p inhibitor in LSECs. (H) VWF mRNA expression was examined by quantitative real-time PCR with the transfection of miR-671-5p inhibitor in LSECs. Data are presented as the mean ± SEM (n = 3 per group). All results were verified in at least three independent experiments. $*P < 0.05$ versus control. $**P < 0.01$ versus control; $^{\#}P < 0.05$ versus S1P-treated or TGFβ1-treated alone; $^{\#\#}P < 0.01$ versus S1P-treated or TGFβ1-treated alone.

Luciferase reporter assays were performed to validate that Angpt1 and VWF were the direct targets of miR-671-5p. Luciferase reporter genes were constructed using the Angpt1 or VWF 3′-UTR and the mutant counterpart at the miR-671-5p binding regions, and then miR-671-5p mimic was co-transfected into the HEK293T cells. The results showed that miR-671-5p overexpression significantly inhibited the luciferase activity of Angpt1 with the wild-type 3′-UTR, but not with mutant 3′-UTR (Fig. 5A). Similar results were obtained with VWF (Fig. 5B). These results provided evidence that Angpt1 and VWF were both direct and functional downstream targets of miR-671-5p.

We also evaluated the effect of miR-671-5p on HSC migration using Transwell chambers and proliferation using the Cell Counting Kit-8 assay. The migration and proliferation ability of HSCs was unchanged in the presence of miR-671-5p mimics in S1P-treated cells (Supporting Fig. S1).

MiR-671-5p ATTENUATED LIVER ANGIOGENESIS BY TARGETING Angpt1 AND VWF *IN VIVO*

The regulation of miR-671-5p on the expression of Angpt1 and VWF and liver angiogenesis was further confirmed *in vivo* through the injection of miR-671-5p agomir (mimic *in vivo*, 5 or 10 nmol/ mouse) into CCl_4-treated mice for 28 days. FACS was performed to sort HSC (PDGFRβ$^+$) and EC/LSEC (CD31$^+$) among liver nonparenchymal cells to confirm the successful induction of miR-671-5p in HSCs and EC/LSEC after the administration of miR-671-5p agomir, verifying the effectiveness and specificity of miRNA agomir in these two cell types *in vivo* (Fig. 6A). The expression of miR-671-5p in liver was also up-regulated, examined by quantitative real-time PCR (Fig. 6A). Then the mRNA expression of target genes Angpt1 and VWF was analyzed by quantitative

real-time PCR, showing that the hepatic Angpt1 (Fig. 6B) and VWF (Fig. 6C) mRNA levels were significantly reduced in a dose-dependent manner after the injection of miR-671-5p agomir in CCl_4-treated mice. The mRNA expression of additional pro-angiogenic markers, including VEGFa (Fig. 6D), Tie2 (Fig. 6E) and FGF (Fig. 6F), was also markedly declined after the administration of miR-671-5p agomir in CCl_4 mice, suggesting the alleviation of pathological angiogenesis after miR-671-5p administration.

The protein expression of Angpt1 presented a similar drop in the presence of miR-671-5p agomir in CCl_4-treated mice (Fig. 7A). The protein level of VWF was also markedly declined after miR-671-5p agomir administration in CCl_4 mice (Fig. 7B). In addition, immunofluorescent staining for CD31 showed the decreasing density of newly formed vessels after the administration of miR-671-5p agomir in CCl_4-treated mice (Fig. 7C,D). Altogether, these results confirmed that miR-671-5p targeted Angpt1 and VWF and attenuated liver angiogenesis *in vivo*.

MiR-671-5p ATTENUATED LIVER FIBROSIS BY TARGETING Angpt1 AND VWF *IN VIVO*

To investigate the potential role of miR-671-5p in liver injury, we undertook correlation analysis to determine the relationship between miR-671-5p and liver fibrosis markers. There was a negative correlation between the hepatic expression of miR-671-5p and fibrosis markers, including α-SMA, Colα1(I), and Colα1(III) in CCl_4-treated liver injury mice (Table 1). Consistently, a negative correlation between miR-671-5p and fibrosis markers in human liver was obtained as well (Table 1). These results indicate the potential role of miR-671-5p in liver fibrosis, which might result from its effect on Angpt1/VWF-mediated angiogenesis.
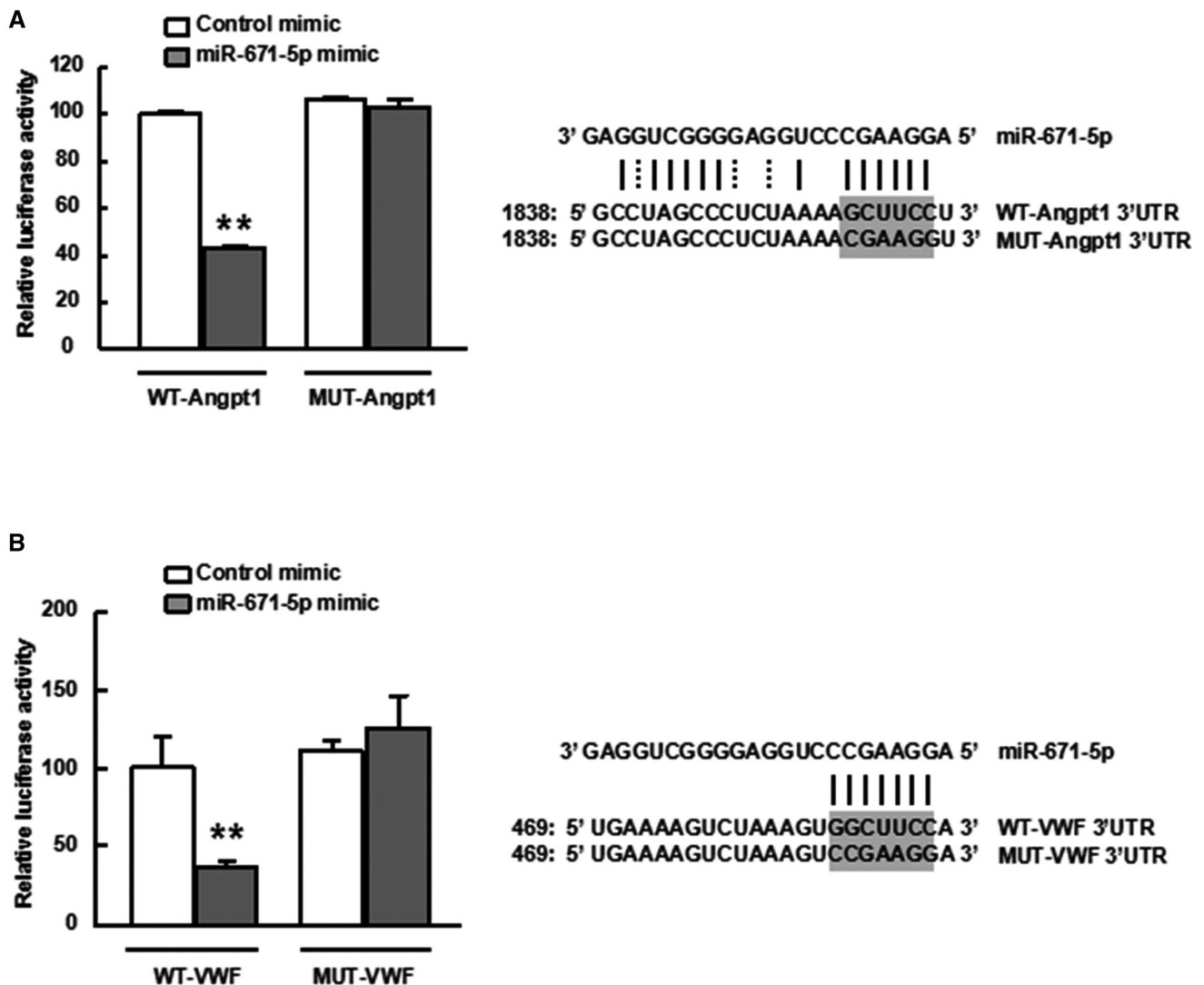
FIG. 5. MiR-671-5p directly targeted Angpt1 and VWF. (A) Luciferase reporter assay to demonstrate Angpt1 was a target of miR-671-5p. (B) Luciferase reporter assay to demonstrate VWF was a target of miR-671-5p. Data are presented as the mean ± SEM (n = 3 per group). All results were verified in at least three independent experiments. $^{**}P < 0.01$ versus control.

Based on these results, we examined the degree of liver fibrosis after the administration of miR-671-5p agomir in CCl_4-treated mice. The mRNA expression of typical fibrosis markers, including α-SMA (Fig. 8A), Colα1(I) (Fig. 8B), and Colα1(III) (Fig. 8C) in liver, was markedly suppressed in the presence of different dosages of miR-671-5p agomir compared with that in CCl_4-treated mice. Hepatic collagen deposition was further evaluated by morphometric analysis of sirius red staining (Fig. 8D) and quantified by digital image analysis, showing that area of collagen deposition was dramatically reduced after the administration of miR-671-5p agomir in CCl_4-treated mice (Fig. 8E). The serum biochemical parameters (alanine aminotransferase and aspartate aminotransferase) were also significant inhibited in the presence of miR-671-5p agomir compared with that in CCl_4-treated mice (Fig. 8F). In addition, we performed another experimental model of liver fibrosis by BDL operation to verify the anti-angiogenic and antifibrotic effects of miR-671-5p agomir. Similar to the results in CCl_4 mice, administration
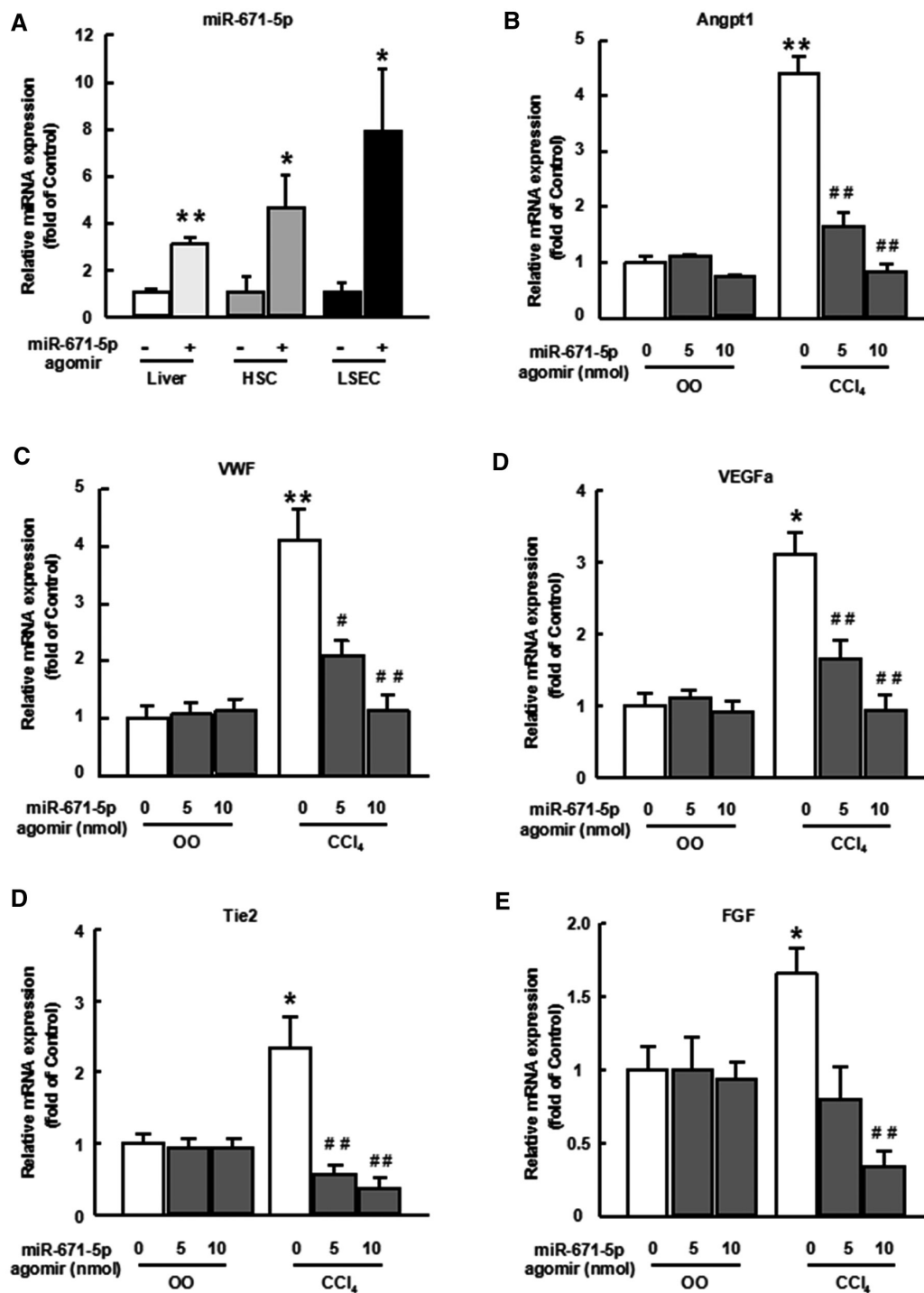
FIG. 6. Effect of miR-671-5p on liver angiogenesis *in vivo*. A total of 5 or 10 nmol/ mouse miR-671-5p agomir (mimic *in vivo*) or agomir negative control was injected into the tail vein twice per week in 28-day CCl_4 mice. (A) The expression of miR-671-5p in liver, sorted HSC, and EC/LSEC after the administration of miR-671-5p agomir in CCl_4 mice. (B) Angpt1 mRNA levels in liver tissue were measured by quantitative real-time PCR with or without miR-671-5p agomir injection in CCl_4 mice. (C) VWF mRNA levels in liver tissue were measured by quantitative real-time PCR. The mRNA expression of VEGFa (D), Tie2 (E), and FGF (F) after the administration of miR-671-5p agomir in CCl_4 mice. Data are presented as the mean ± SEM (n = 6 per group). *$P < 0.05$ versus control; **$P < 0.01$ versus control; [#]$P < 0.05$ versus CCl_4-treated alone. [##]$P < 0.01$ versus CCl_4-treated alone.

FIG. 7. Effect of miR-671-5p on liver angiogenesis *in vivo*. miR-671-5p agomir (mimic *in vivo*) or agomir negative control was injected into the tail vein twice per week in 28-day CCl_4 mice. (A) Angpt1 protein levels in liver tissue were measured by western blot. (B) VWF protein levels in liver tissue were measured by western blot. (C) Representative images of immunofluorescence analysis to track CD31 (red) expression in the fibrotic liver. (D) The number of CD31-positive cells per field was calculated by Image-Pro Plus software. Data are presented as the mean ± SEM (n = 6 per group). **P < 0.01 versus control; ##P < 0.01 versus CCl_4-treated alone.

of miR-671-5p agomir also resulted in the attenuation of liver angiogenesis and fibrosis in BDL mouse models *in vivo* (Supporting Fig. S2). Taken together, these results suggest that the regulation of miR-671-5p on Angpt1/VWF and liver angiogenesis led to the attenuation of liver fibrosis *in vivo*.
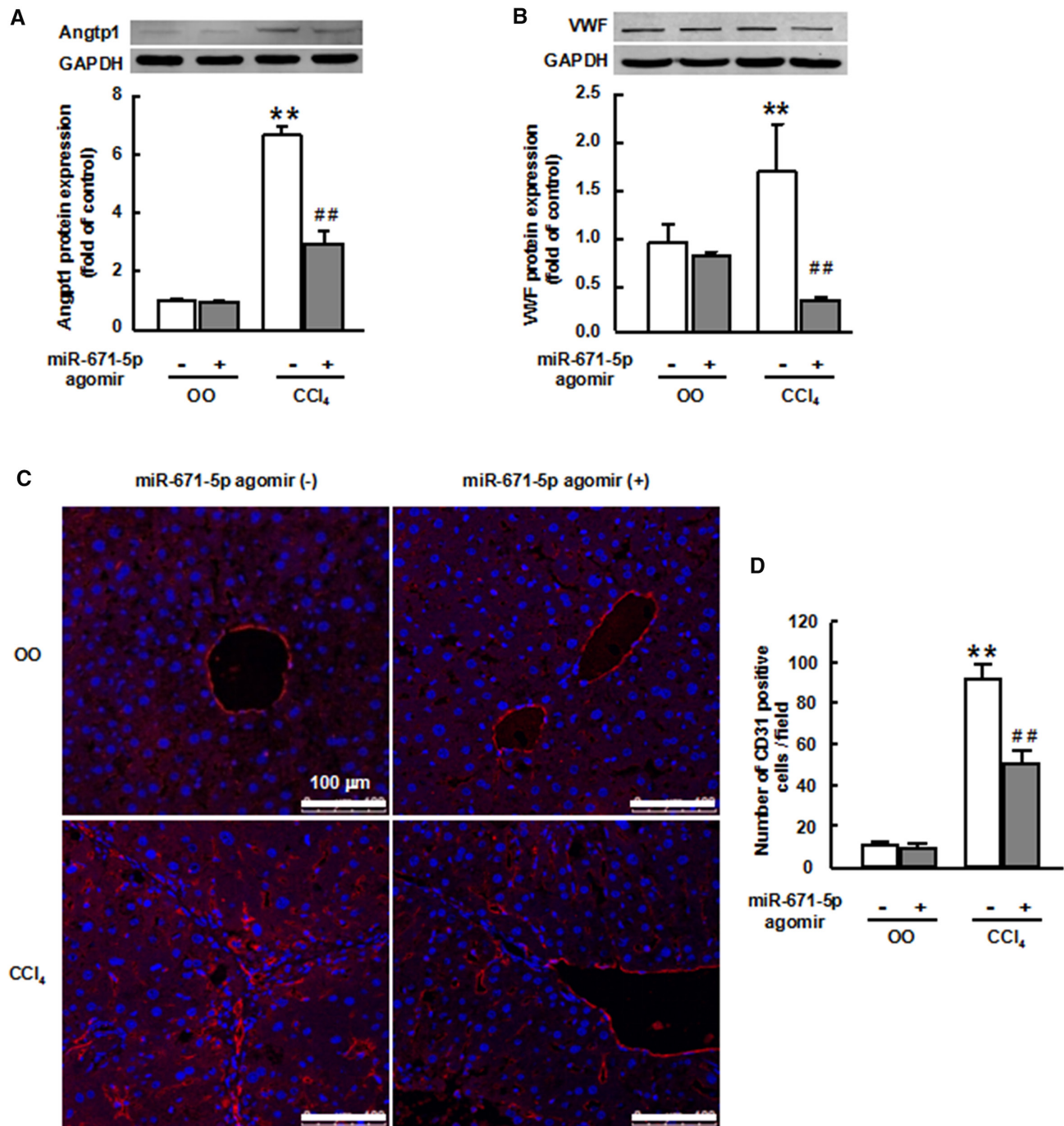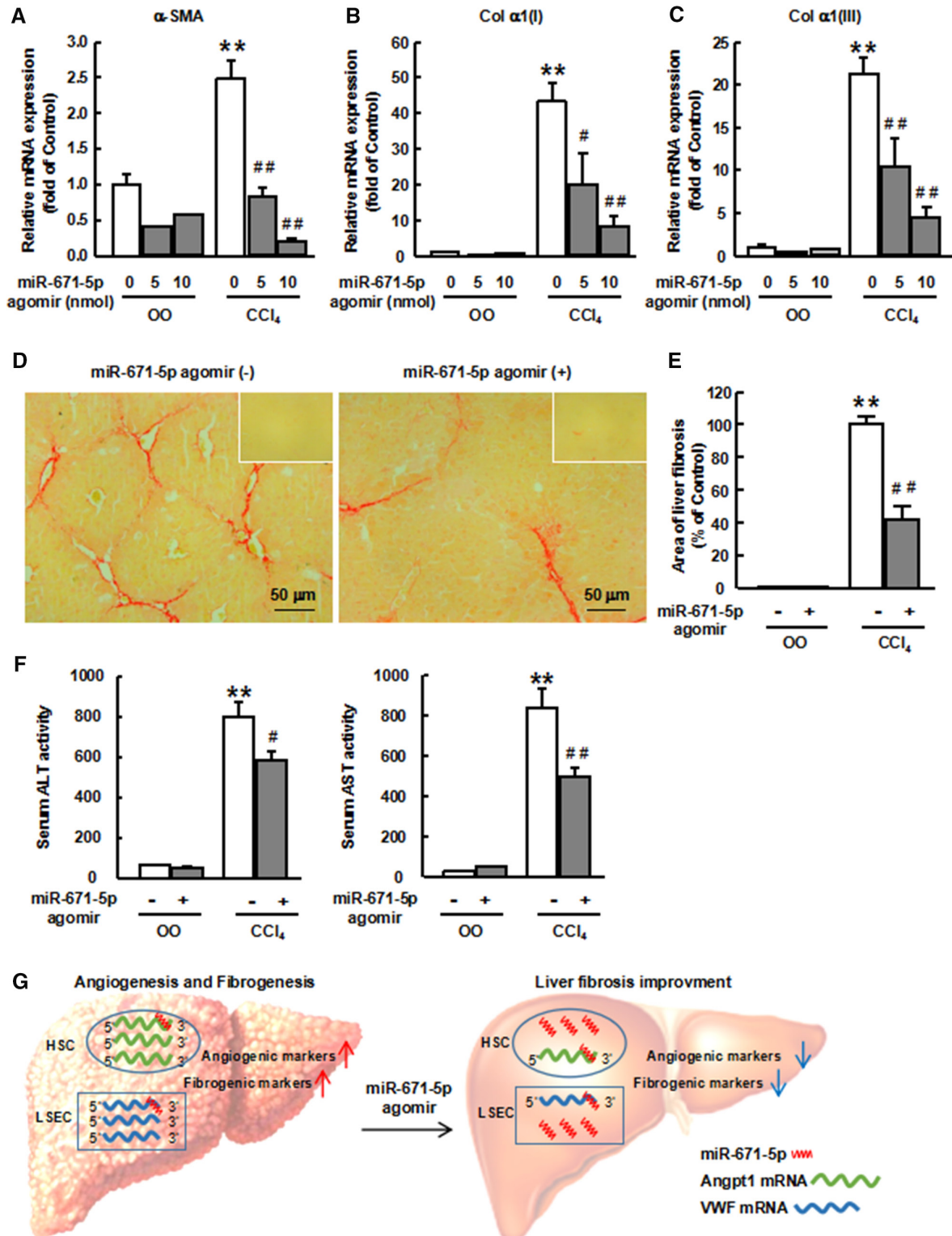
FIG. 8. Effect of miR-671-5p on liver fibrosis *in vivo*. miR-671-5p agomir (mimic *in vivo*) or agomir negative control was injected into the tail vein twice per week in 28-day CCl_4 mice. The mRNA levels of fibrosis markers, including α-SMA (A), Colα1(I) (B), and Col α1(III) (C), in the fibrotic liver with the injection of miR-671-5p agomir was measured by quantitative real-time PCR. (D) Representative sirius red–stained liver sections and quantification of fibrotic areas in CCl_4 mice with the injection of miR-671-5p agomir. Inset: Sirius red staining for control livers. (E) Quantitation of collagen deposition by sirius red staining. (F) Serum alanine aminotransferase and aspartate aminotransferase activity in CCl_4 mice with or without the injection of miR-671-5p agomir. (G) Summary of the overall findings. Data are presented as the mean ± SEM (n = 6 per group). **$P < 0.01$ versus control; #$P < 0.05$ versus CCl_4-treated alone; ##$P < 0.01$ versus CCl_4-treated alone. Abbreviations: ALT, alanine aminotransferase; AST, aspartate aminotransferase.

Discussion

Here we explore the potential role of miR-671-5p in liver fibrosis–associated angiogenesis by directly targeting Angpt1 and VWF. The present work provides several findings (Fig. 8G): (1) MiR-671-5p is decreased in the fibrotic liver of human and mice, with a negative correlation with Angpt1 and VWF levels; (2) MiR-671-5p, which displays a significant decrease in activated HSCs and LSECs, directly targets Angpt1 and VWF by the transfections of miR mimics/inhibitors and luciferase reporter assays; and (3) *in vivo* miR-671-5p agomir negatively regulates the expression of Angpt1 and VWF, resulting in the alleviation of liver angiogenesis and fibrosis in CCl_4-treated and BDL mice.

Recent studies have reported that miR-671-5p plays a critical role in multiple biological processes. For instance, miR-671-5p promotes prostate cancer cell proliferation by inhibiting SRY (sex determining region Y)-box 6.[25] Long noncoding Rpa and circular Rar1 jointly target miR-671-5p to promote neuronal apoptosis through up-regulation of the pro-apoptotic proteins caspase8 and p38 in lead-induced neuronal apoptosis.[26] MiR-671-5p influences nucleotide-binding oligomerization domain containing 2 gene expression as well as its downstream nuclear factor kappa B activity and immune responses in intestinal epithelial cells.[27] MiR-671 serves as a prognostic biomarker for patients with kidney cancer, with wild-type breast cancer 1–associated protein-1.[28] However, the functional role of miR-671-5p in liver disease is unclear up until now. In the current study, we document the role of miR-671-5p in liver fibrosis and angiogenesis by targeting two important angiogenic molecules, Angpt1 and VWF, showing that miR-671-5p overexpression remarkably inhibits the up-regulation of Angpt1 and VWF and attenuates liver fibrosis and angiogenesis in CCl_4-treated mice. Here we display the decreased expression of

miR-671-5p in injured liver and the negative correlation between the expression of Angpt1 and miR-671-5p, and VWF and miR-671-5p, in both mouse and human liver. In our study, mouse liver injury models are induced by CCl_4 injection or BDL operation, which are two typical liver injury models.[29] Human liver samples are obtained from patients with chronic liver disease of different etiologies, including chronic HBV, HCV infections, alcohol-associated liver disease, cryptogenic liver disease, cholestatic liver disease, drug-induced liver disease, and autoimmune liver disease. Thus, our results reveal the universal regulation of miR-671-5p on angiogenesis regardless of species and the etiology of liver diseases, suggesting the great potential of miR-671-5p/Angpt1 and miR-671-5p/VWF-based intervention targets for liver diseases. As for the upstream cause of miR-671 dysregulation, there have been few published reports discussing this question. We demonstrated that *in vitro* S1P stimulation decreased miR-671-5p expression in a dose-dependent manner in HSCs, whereas TGFβ1 treatment down-regulated miR-671-5p expression in LSECs. *In vivo*, we speculated that multiple liver injury–related factors or signals could be contributing to the mechanism controlling miR-671 dysregulation in the complex internal environment of fibrotic liver. Therefore, further studies will be needed to establish this issue.

Liver fibrosis and pathological angiogenesis are interdependent processes that occur in parallel.[30] During hepatic fibrogenesis, new vascular structures are formed to provide oxygen and nutrients to areas of active scarring and tissue remodeling, thereby driving chronic inflammation and fibrosis progression.[31] In the present study, protein–protein interaction network by STRING shows the close relationship between angiogenesis and liver fibrosis, and the participation of S1P system in the network of Angpt1-mediated and VWF-mediated angiogenesis. At the molecular level, angiogenesis results

from an imbalance between drivers of vessel growth and maturation (e.g., angiopoietin, VEGF, FGF, platelet-derived growth factor, hepatocyte growth factor, endoglin) and inhibitors (e.g., angiostatin, endostatin, thrombospondin-1).[32,33] Angpt1, a member of angiopoietin family, has been proved to be a critical driver in liver fibrosis–associated angiogenesis in mouse fibrotic liver by our previous study,[8] and its mechanism of action is analyzed in the present study, which is associated with miR-671-5p. Angpt1 is a secretory ligand of tyrosine kinase with immunoglobulin and epidermal growth factor homology domain 2 (Tie2), which is primarily expressed by vascular endothelial cells, and Angpt1/Tie2 pathways are crucial for vascular maturation and stability.[34-36] Further studies are required to establish the effect of Tie2 receptor on Angpt1-drived angiogenesis during liver injury.

HSCs, which have been well established as collagen-producing cells in liver, are increasingly recognized for their role in angiogenesis and vascular remodeling during liver disease.[37,38] In fact, HSCs are recognized as liver-specific pericytes that are dispersed along the sinusoids with spatial extensions, and thus are sufficient to cover the entire sinusoidal microcirculatory network.[39,40] They are able to participate in angiogenesis and contribute to the development of liver fibrosis by directly secreting pro-angiogenic cytokines Angpt1.[39,40] Here we investigate the mechanisms underlying the angiogenic role of HSCs mediated by Angpt1, and identify a key role for miR-671-5p in this context. In addition, we find that miR-671-5p also exerts a negative regulatory effect on VWF, which is primarily expressed by endothelial cells and has been used extensively to quantify angiogenesis in a variety of tumors.[41] Given the close anatomic relationship between HSCs and sinusoidal endothelial cells, the interaction of HSCs with endothelial cells needs to be further explored.

Altogether, we identify the negative regulation of miR-671-5p on its targets Angpt1 and VWF in liver fibrosis–associated angiogenesis, which may open new perspectives for pharmacological treatment of liver disease.

REFERENCES

1) Pellicoro A, Ramachandran P, Iredale JP, Fallowfield JA. Liver fibrosis and repair: immune regulation of wound healing in a solid organ. Nat Rev Immunol 2014;14:181-194.

2) Tacke F, Trautwein C. Mechanisms of liver fibrosis resolution. J Hepatol 2015;63:1038-1039.

3) Parikh SM. Angiopoietins and Tie2 in vascular inflammation. Curr Opin Hematol 2017;24:432-438.

4) Aguilera KY, Brekken RA. Recruitment and retention: factors that affect pericyte migration. Cell Mol Life Sci 2014;71:299-309.

5) Lamalice L, Le Boeuf F, Huot J. Endothelial cell migration during angiogenesis. Circ Res 2007;100:782-794.

6) Randi AM, Smith KE, Castaman G. von Willebrand factor regulation of blood vessel formation. Blood 2018;132:132-140.

7) Peyvandi F, Kouides P, Turecek PL, Dow E, Berntorp E. Evolution of replacement therapy for von Willebrand disease: from plasma fraction to recombinant von Willebrand factor. Blood Rev 2019;38:100572.

8) Yang L, Yue S, Yang L, Liu X, Han Z, Zhang Y, et al. Sphingosine kinase/sphingosine 1-phosphate (S1P)/S1P receptor axis is involved in liver fibrosis-associated angiogenesis. J Hepatol 2013;59:114-123.

9) Yang L, Tian L, Zhang Z, Zhou X, Ji X, Liu F, et al. Cannabinoid receptor 1/miR-30b-5p axis governs macrophage NLRP3 expression and inflammasome activation in liver inflammatory disease. Mol Ther Nucleic Acids 2020;20:725-738.

10) Pu M, Chen J, Tao Z, Miao L, Qi X, Wang Y, et al. Regulatory network of miRNA on its target: coordination between transcriptional and post-transcriptional regulation of gene expression. Cell Mol Life Sci 2019;76:441-451.

11) Sun Z, Shi KE, Yang S, Liu J, Zhou Q, Wang G, et al. Effect of exosomal miRNA on cancer biology and clinical applications. Mol Cancer 2018;17:147.

12) Dong H, Weng C, Bai R, Sheng J, Gao X, Li L, et al. The regulatory network of miR-141 in the inhibition of angiogenesis. Angiogenesis 2019;22:251-262.

13) Zhang D, Lee H, Wang X, Rai A, Groot M, Jin Y. Exosome-mediated small RNA delivery: a novel therapeutic approach for inflammatory lung responses. Mol Ther 2018;26:2119-2130.

14) Wang X, He Y, Mackowiak B, Gao B. MicroRNAs as regulators, biomarkers and therapeutic targets in liver diseases. Gut 2021;70:784-795.

15) Ezaz G, Trivedi HD, Connelly MA, Filozof C, Howard K, L.Parrish M, et al. Differential associations of circulating MicroRNAs with pathogenic factors in NAFLD. Hepatol Commun 2020;4:670-680.

16) Yang X, Zhang X-F, Lu XU, Jia H-L, Liang L, Dong Q-Z, et al. MicroRNA-26a suppresses angiogenesis in human hepatocellular carcinoma by targeting hepatocyte growth factor-cMet pathway. Hepatology 2014;59:1874-1885.

17) Wang R, Zhao NA, Li S, Fang J-H, Chen M-X, Yang J, et al. MicroRNA-195 suppresses angiogenesis and metastasis of hepatocellular carcinoma by inhibiting the expression of VEGF, VAV2, and CDC42. Hepatology 2013;58:642-653.

18) Zeng Z, Li Y, Pan Y, Lan X, Song F, Sun J, et al. Cancer-derived exosomal miR-25-3p promotes pre-metastatic niche formation by inducing vascular permeability and angiogenesis. Nat Commun 2018;9:5395.

19) Yang L, Dong C, Yang J, Yang L, Chang N, Qi C, et al. MicroRNA-26b-5p inhibits mouse liver fibrogenesis and angiogenesis by targeting PDGF receptor-beta. Mol Ther Nucleic Acids 2019;16:206-217.

20) Li C, Jiang X, Yang L, Liu X, Yue S, Li L. Involvement of sphingosine 1-phosphate (SIP)/S1P3 signaling in cholestasis-induced liver fibrosis. Am J Pathol 2009;175:1464-1472.

21) Han Z, Zhu T, Liu X, Li C, Yue S, Liu X, et al. 15-deoxy-delta ^{12,14}-prostaglandin J2 reduces recruitment of bone marrow-derived monocyte/macrophages in chronic liver injury in mice. Hepatology 2012;56:350-360.

22) Pugh CW, Ratcliffe PJ. Regulation of angiogenesis by hypoxia: role of the HIF system. Nat Med 2003;9:677-684.

23) Hisano Y, Hla T. Bioactive lysolipids in cancer and angiogenesis. Pharmacol Ther 2019;193:91-98.

24) Yang LE, Chang NA, Liu X, Han Z, Zhu T, Li C, et al. Bone marrow-derived mesenchymal stem cells differentiate to hepatic myofibroblasts by transforming growth factor-β1 via sphingosine kinase/sphingosine 1-phosphate (S1P)/S1P receptor axis. Am J Pathol 2012;181:85-97.

25) Yu Y, Wang Z, Sun D, Zhou X, Wei X, Hou W, et al. miR-671 promotes prostate cancer cell proliferation by targeting tumor suppressor SOX6. Eur J Pharmacol 2018;823:65-71.

26) Nan A, Chen L, Zhang N, Liu Z, Yang TI, Wang Z, et al. A novel regulatory network among LncRpa, CircRar1, MiR-671 and apoptotic genes promotes lead-induced neuronal cell apoptosis. Arch Toxicol 2017;91:1671-1684.

27) Chuang AY, Chuang JC, Zhai Z, Wu F, Kwon JH. NOD2 expression is regulated by microRNAs in colonic epithelial HCT116 cells. Inflamm Bowel Dis 2014;20:126-135.

28) **Ge YZ**, **Xu LW**, **Zhou CC**, Lu TZ, Yao WT, Wu R, et al. A BAP1 mutation-specific MicroRNA signature predicts clinical outcomes in clear cell renal cell carcinoma patients with wild-type BAP1. J Cancer 2017;8:2643-2652.

29) **Li C**, **Kong Y**, **Wang H**, Wang S, Yu H, Liu X, et al. Homing of bone marrow mesenchymal stem cells mediated by sphingosine 1-phosphate contributes to liver fibrosis. J Hepatol 2009;50:1174-1183.

30) Medina J, Arroyo AG, Sanchez-Madrid F, Moreno-Otero R. Angiogenesis in chronic inflammatory liver disease. Hepatology 2004;39:1185-1195.

31) Hammoutene A, Rautou PE. Role of liver sinusoidal endothelial cells in nonalcoholic fatty liver disease. J Hepatol 2019;70:1278-1291.

32) Morse MA, Sun W, Kim R, He AR, Abada PB, Mynderse M, et al. The role of angiogenesis in hepatocellular carcinoma. Clin Cancer Res 2019;25:912-920.

33) **Zhang Y**, **Yang Y**, Hosaka K, Huang G, Zang J, Chen F, et al. Endocrine vasculatures are preferable targets of an antitumor ineffective low dose of anti-VEGF therapy. Proc Natl Acad Sci U S A 2016;113:4158-4163.

34) Yin GN, Jin H-R, Choi M-J, Limanjaya A, Ghatak K, Minh NN, et al. Pericyte-derived Dickkopf2 regenerates damaged penile neurovasculature through an angiopoietin-1-Tie2 pathway. Diabetes 2018;67:1149-1161.

35) Slater SC, Jover E, Martello A, Mitić T, Rodriguez-Arabaolaza I, Vono R, et al. MicroRNA-532-5p regulates pericyte function by targeting the transcription regulator BACH1 and angiopoietin-1. Mol Ther 2018;26:2823-2837.

36) Koh GY. Orchestral actions of angiopoietin-1 in vascular regeneration. Trends Mol Med 2013;19:31-39.

37) Shao S, Duan W, Xu Q, Li X, Han L, Li W, et al. Curcumin suppresses hepatic stellate cell-induced hepatocarcinoma angiogenesis and invasion through downregulating CTGF. Oxid Med Cell Longev 2019;2019:8148510.

38) **Ceni E**, **Mello T**, Polvani S, Vasseur-Cognet M, Tarocchi M, Tempesti S, et al. The orphan nuclear receptor COUP-TFII coordinates hypoxia-independent proangiogenic responses in hepatic stellate cells. J Hepatol 2017;66:754-764.

39) Zhang F, Hao M, Jin H, Yao Z, Lian N, Wu LI, et al. Canonical hedgehog signalling regulates hepatic stellate cell-mediated angiogenesis in liver fibrosis. Br J Pharmacol 2017;174:409-423.

40) Lee JS, Semela D, Iredale J, Shah VH. Sinusoidal remodeling and angiogenesis: a new function for the liver-specific pericyte? Hepatology 2007;45:817-825.

41) Vermeulen PB, Gasparini G, Fox SB, Toi M, Martin L, Mcculloch P, et al. Quantification of angiogenesis in solid human tumours: an international consensus on the methodology and criteria of evaluation. Eur J Cancer 1996;32A:2474-2484.

Author names in bold designate shared co-first authorship.

Supporting Information

Additional Supporting Information may be found at onlinelibrary.wiley.com/doi/10.1002/hep4.1888/suppinfo.